Automatizing the broken bar detection process via Short Time Fourier Transform and two-dimensional Piecewise Aggregate Approximation representation

George Georgoulas, Petros Karvelis, Chysostomos D. Stylios
Laboratory of Knowledge and Intelligent Computing,
Department of Computer Engineering,
TEI of Epirus,
47100 Artas, Kostakioi, Greece
georgoul@kic.teiep.gr, pkarvelis@kic.teiep.gr,
stylios@teiep.gr

Ioannis P. Tsoumas
Larges Drives R&D Department
Siemens Industry Sector - Drive Technologies
Nuremberg, Germany
ytsoumas@ieee.com

Jose Alfonso Antonino-Daviu, Vicente Climente-Alarcon
Instituto de Ingeniería Energética
Universitat Politècnica de València
Valencia, Spain
joanda@die.upv.es, viclial@ieee.org

Abstract—**This work presents an automated approach for detecting broken rotor bars in induction machines using the stator current during startup operation. The currents are analyzed using the well-known Short Time Fourier Transform (STFT) producing a two-dimensional time-frequency representation. This representation contains information regarding the presence of a characteristic transient component but requires further processing before it can be fed into a standard classification algorithm. In this work, this part is performed using the two dimensional extension of Piecewise Aggregate Approximation (PAA) that can deal with the two dimensional representation of STFT. The results (with both simulated and experimental data) suggest that the method can be used for the automatic detection of broken bars and even for determining the fault severity. Moreover, its low computational burden makes it ideal for its future use in on-line, unsupervised systems, as well as in portable condition monitoring devices**

I. INTRODUCTION

These recent decades have lived huge advances in the electric machines fault diagnosis area. This has been partially due to the extrapolation to this area of advanced artificial intelligence, signal processing and pattern recognition techniques that have been successfully applied in other scientific fields [1]. In this context, a significant proliferation of fault diagnosis techniques relying on sophisticated time-frequency decomposition tools (wavelet transforms, Wigner-Ville or Choi-Williams Distributions, Hilbert-Huang transforms, Hilbert transforms, etc...) [2]] has been observed.

Many of the aforementioned methods have been applied to the detection of a certain variety of faults (stator short-circuits, rotor damages, bearing faults, eccentricities, etc...) in different types of machines (either DC or AC). In this regard, the detection of rotor faults has drawn a substantial attention. Though this is not among the most common faults in AC motors, its relatively simple detection through its signatures in the current spectrum, as well as its higher importance and occurrence rate in large motors (often the most critical, expensive and difficult to repair) have justified the deep study of this fault in the literature as well as the development of suitable fault detection techniques [3].

However, in spite of this prolific activity, the classical Motor Current Signature Analysis (MCSA) is still predominantly used in many industrial sites as well as by most of the few available condition monitoring devices to assess the rotor condition [6]. MCSA has however, important drawbacks, as extensively reported by several authors, such as the incorrect diagnostic results of this tool (either false negatives or false positives), that can have to huge economic repercussions [7].

These problems of MCSA have justified the attempts to promote the industrial penetration of some advanced techniques. Indeed, some of them can avoid some of the MCSA constraints, increasing the reliability of the diagnostic, as reported in several works.

In this context, the analysis of startup current (that is commonly referred as Transient-MCSA) using advanced signal processing tools has been proven to be especially

978-1-4799-5776-7/14/$31.00 ©2014 IEEE

suitable to this end; the fault-associated patterns appearing in the resulting time-frequency maps are very unlikely to be caused by a different phenomenon or reason, a fact that justifies its use, especially in controversial cases in which application of MCSA is not suitable [7].

In spite of the advances in this area, most of these techniques still rely on a qualitative interpretation of the resulting patterns that must be carried out by an expert user [11]. In other words, it is not feasible yet the implementation of these techniques in unsupervised systems that do not require the human intervention, a fact that would facilitate the penetration of these techniques in the industrial world.

This work proposes a new, computationally efficient method to automatize the detection process of rotor faults, based on the representation resulting from application of a very simple time-frequency tool (STFT) on the startup current. The high-dimensional output of the STFT requires a data-reduction method before it can be used by a classification algorithm. In this work two-dimensional PAA [12] is employed to reduce the dimensionality of the original STFT representation. Then a typical pattern recognition approach is utilized for the final diagnosis involving an unsupervised dimensionality reduction stage based on Principal Component Analysis (PCA) and a simple linear classifier.

The application of the method to signals obtained from simulation as well as experiment demonstrates that the methodology does not only allow to detect the fault, but also to determine its severity with high accuracy.

The rest of the paper is structured as follows: Section II describes the overall procedure with special emphasis given to the PAA variants. In Section III the evaluation procedure is summarized along with the achieved results while Section IV concludes the paper offering also some insights for future research.

II. Procedure

The overall procedure is depicted in Figure 1. The procedure is basically based on the analysis of the stator current using STFT and then the application of the two-dimensional PAA. However, it also includes a stage for the isolation of the transient before the application of the STFT as well as a dimensionality reduction stage following the PAA stage and a final stage consisting of a conventional classifier. The rest of this section describes each one of these stages.

A. Transient Isolation

The proposed approach belongs to the Transient MCSA methods. As a result the steady state operation should be discarded. A steady state detector [14] based on the Root Mean Square (RMS) value of the acquired line current calculated over a sliding window was used to select the portion of the signal that should be retained.

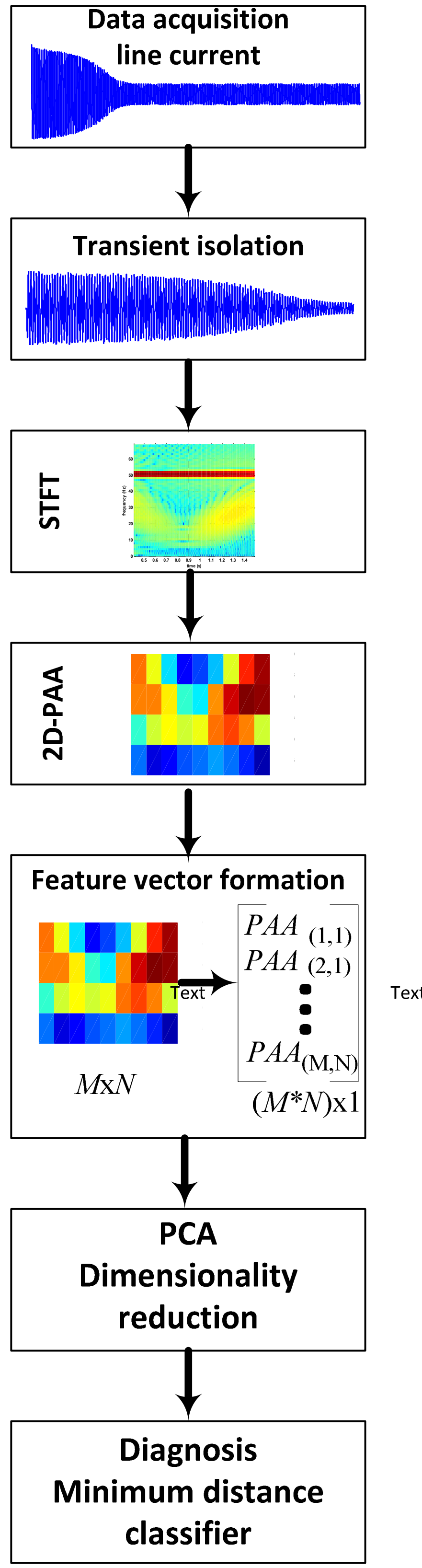

Figure 1. The overall procedure: from data acquisition to condition assessment

The “running” standard deviation of the “running” RMS was computed again using a second sliding window and once its value was fallen below a predefined limit, the end of the transient was declared.

B. *Time-frequency representation*

After the isolation of the transient, STFT was employed to produce the time-frequency representation of the original signal.

STFT is probably the simplest method for rendering time-frequency information from a signal $x(t)$ and it consists of the application of the Fourier transform over a sliding window $w(t)$ applied on $x(t)$.

$$X(t,\omega)=\int_{-\infty}^{\infty} x(\tau)w(\tau-t)e^{-j\omega\tau}d\tau \qquad (1)$$

STFT is very appealing tool, due to its ease of implementation using the Fast Fourier Transform (FFT), a transform which is very familiar to engineers, compared to other more sophisticated time-frequency representations. STFT can capture the presence of the faulty component that manifests itself creating a V-like shape in the spectrogram (the squared amplitude of the output of the STFT) as it can be seen in Fig. 2, which however is smeared across time and frequency, due to the inherent limitations of any method that relies on the FFT [3,8].

So far, most transient analysis methods for the diagnosis of broken bars, rely on sophisticated algorithms to track this specific V-like structure [3,8,11], or its variations [14]. In this work we resort to a much simpler, though quite successful, “less is more” approach for processing the spectrogram. The method is called PAA and it was originally developed for one dimensional data series [12].

C. *Piecewise Aggregate Approximation And Its Two-Dimensional Variant*

PAA is a dimensionality reduction method, where a time series S of length N can be represented in a p-dimensional space by a vector $\bar{S}=\bar{s}_1,\ldots,\bar{s}_p$. The i-th element of S is calculated by the following equation:

$$\bar{s}_i=\frac{p}{N}\sum_{j=\frac{p}{N}(i-1)+1}^{\frac{p}{N}i} s_j \qquad (2)$$

Thus, in order to reduce the time series from N dimensions to p dimensions, the data is divided into p equal sized windows. The mean value of the data falling within a frame is calculated and a vector of these values becomes the data-reduced representation. An illustrative example of the application of PAA to the second Intrinsic Mode Function (IMF) of a start-up current of an induction machine with two broken bars is shown in Fig. 3 [15].

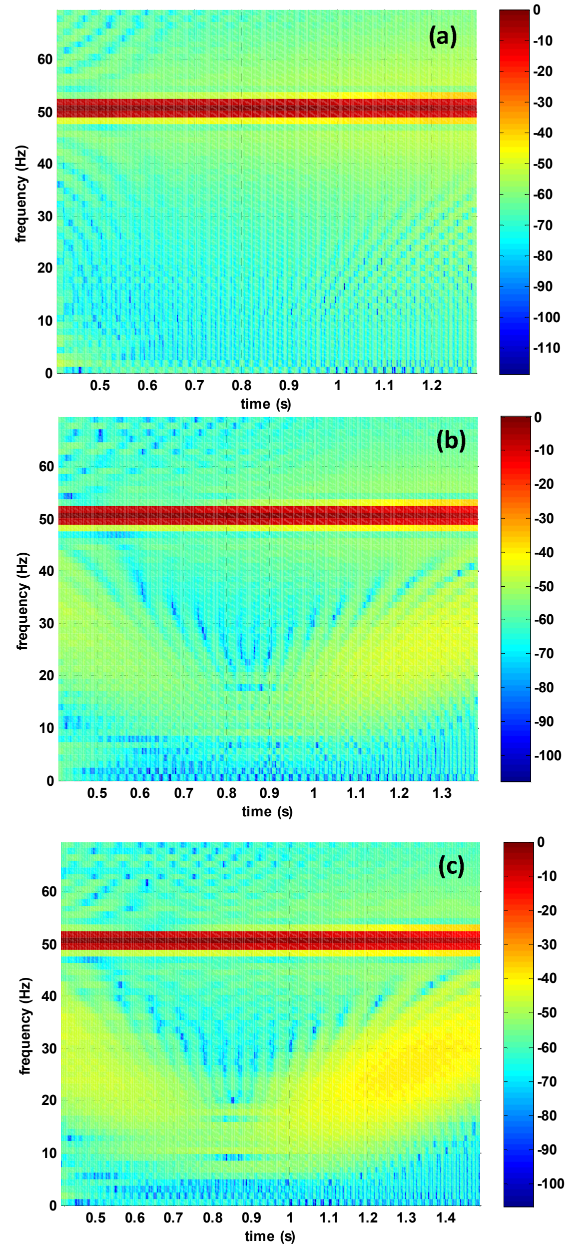

Figure 2. The spectrogram of the start-up current for: a) a healthy machine, b) a machine with one broken bar and c) a machine with two broken bars. The data come from the experimental set-up described in Section III.

The original formulation assumes that the length of the signal (N) is divided exactly by p. Since this is not always the case, an expansion can be derived by accounting for the border line points (having them contribute to the mean value a fraction proportional to the distance from the border line point). Therefore the i-th element of S is now given by the following equation:

$$\bar{s}_i = \frac{p}{N}\left(\left(1-\left(\left(\frac{N}{p}(i-1)+1\right)-\left\lfloor\frac{N}{p}(i-1)+1\right\rfloor\right)\right)\cdot s_{\left\lfloor\frac{N}{p}(i-1)+1\right\rfloor}\right)+$$
$$\frac{p}{N}\left(\sum_{j=\left\lfloor\frac{N}{p}(i-1)+1\right\rfloor+1}^{\left\lfloor\frac{N}{p}i+1\right\rfloor-1} s_j + \left(\left(\left(\frac{N}{p}i+1\right)-\left\lfloor\frac{N}{p}i+1\right\rfloor\right)\cdot s_{\left\lfloor\frac{N}{p}(i)+1\right\rfloor}\right)\right)$$

for $i = 1, 2, ..., p$ (3)

where the symbol $\lfloor x \rfloor$, denotes "the largest integer not greater than x,

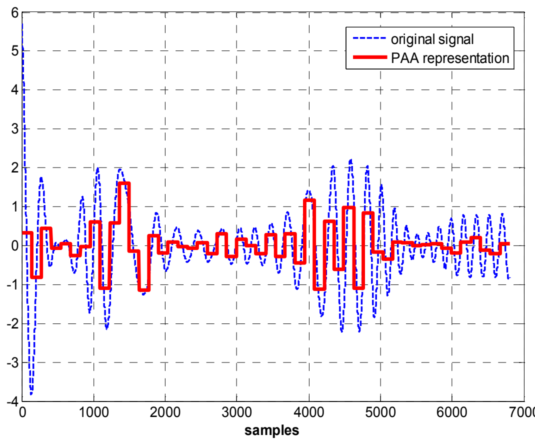

Figure 3. Application of PAA to the second Intrinsic Mode Function (IMF) of a start-up current of an induction machine with two broken bars

The expansion to two dimensions is quite straightforward and has already been used as part of a two-dimensional authentication algorithm [16]. In the two dimensional case the original matrix Q (image) of dimension $N \times M$ is represented by a matrix $\bar{Q}$ of dimension $p_1 \times p_2$ where the $\bar{Q}(i, j)$ element is given by (4):

$$\bar{Q}(i,j) = \frac{1}{p_1 p_2} \sum_{x=\frac{m}{p_1}(i-1)+1}^{\frac{m}{p_1}i} \sum_{y=\frac{n}{p_2}(j-1)+1}^{\frac{n}{p_2}j} Q(x,y) \tag{4}$$

Fig. 4 depicts an illustrative example of the two dimensional PAA process while Fig. 5 shows the corresponding PAA representations of the spectrograms of Fig. 2 (excluding however the upper part of the image- i.e. the frequency components above 45Hz, since the component of interests lies in the lower part of the spectrogram, below the supply frequency of 50 Hz). The reduced PAA representation even though has compressed most of the details present in the original spectrogram still suffices for automatic diagnosis as it is described in the following section.

Practically, the two dimensional PAA can be produced by applying the one dimensional PAA twice: first, applying the PAA along the columns of the matrix reducing the dimension from N to p_1 (new intermediate representation $p_1 \times M$) and then applying the PAA along the rows of the intermediate representation reducing the dimension from M to p_2 producing the final $p_1 \times p_2$ representation. The operations are interchangeable; we can first process the rows and then the columns of the original matrix.

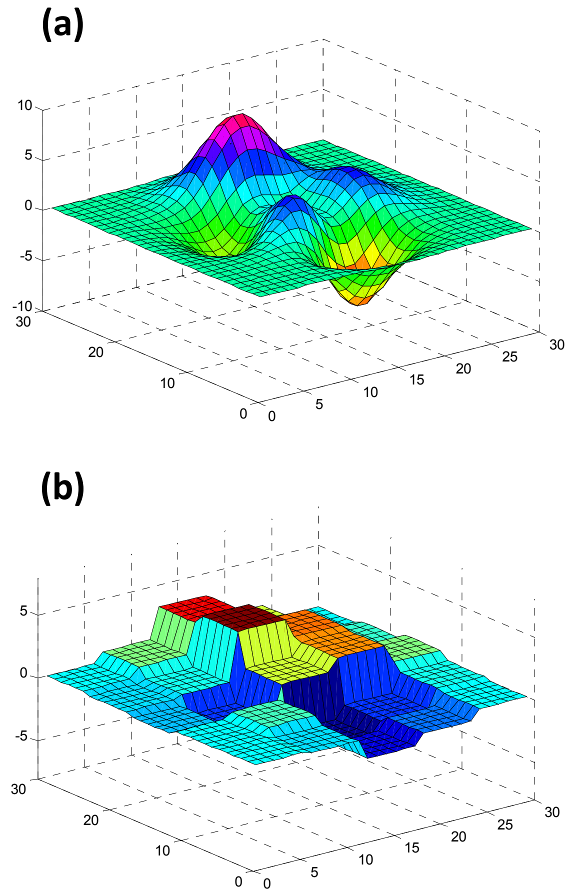

Figure 4. Application of PAA into an image a) the original image (30x30) and b) the reduced representation (5x5) (artificially expanded to span the same range (30x30).

III. Evaluation Of The Method

In order to test the effectiveness of the representation simulation and experimental data were gathered. The simulation data were produced using a squirrel cage asynchronous machine model developed in Matlab/Simulink.

For the experimental part a machine with the following characteristics was used: Rated characteristics of the 1.1 kW motor: Star connection, rated voltage (U_n): 400V, rated power (P_n): 1.1 kW, 2 pair of poles, primary rated current (I_{1n}): 2.7A, rated speed (n_n): 1410 rpm and rated slip (s_n): 0.06. The number of rotor bars is 28. The motor was directly coupled to a DC machine acting as load.

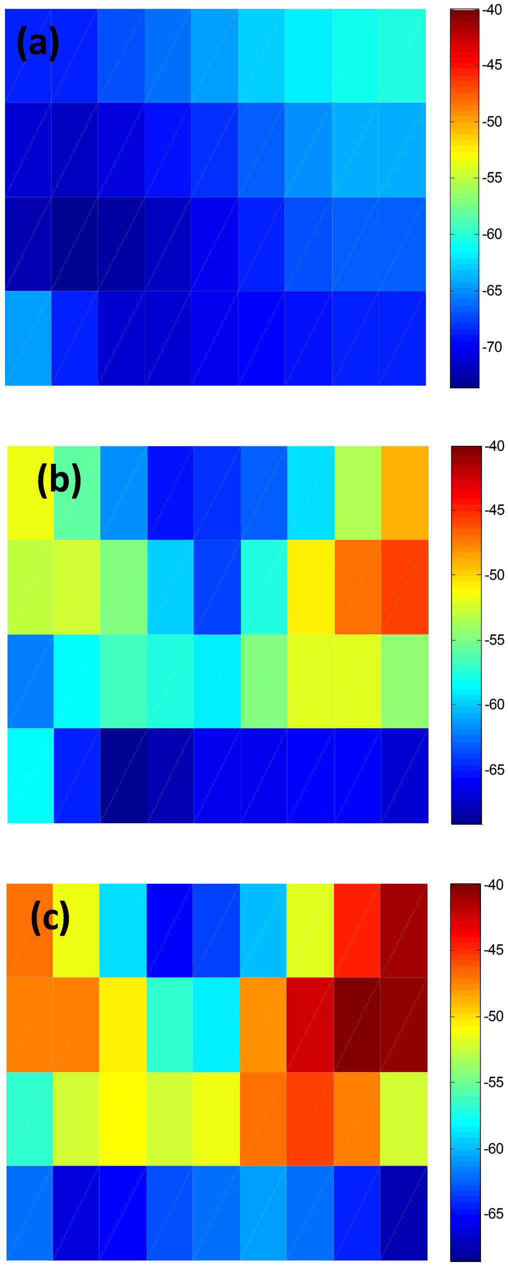

Figure 5. The reduced dimension PAA representation of the lower part of the spectrograms depicted in figure 1 with a 5x10 representation for a) a healthy machine, b) a machine with one broken bar and c) a machine with two broken bars.

The broken bar scenario was "simulated by drilling a hole in the corresponding bar, just in the junction point between the bar and the short-circuit end ring in such a way that the bar had no contact at all with the end-ring (Fig. 6) [8].

Stator currents were sampled with a frequency of 5 kHz. Four experimental start-ups for each condition (twelve in total), two at no load and two at half of the rated load, with different startup durations, were carried out. For the simulation part, ten start-ups were simulated with different durations of the transient phenomenon for each condition (30 in total). For each of the aforementioned cases (simulation and experimental) all three stator currents were recorded.

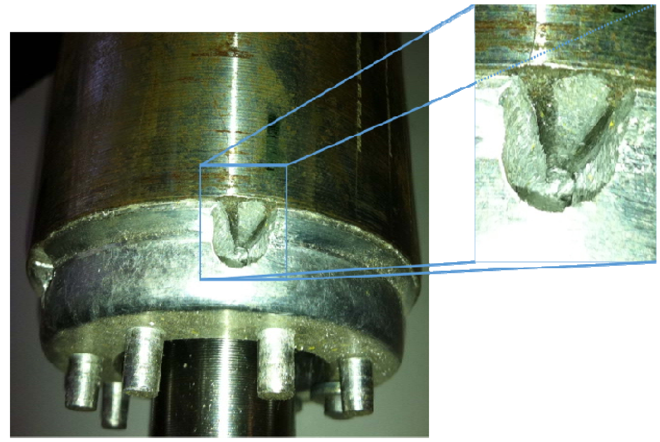

Figure 6. Disassembled rotor with one broken bar.

An initial set of experiments with the simulation data revealed that the reduced dimension of the PAA representation (5x10=50 dimensional space (putting all the elements of the reduced matrix into a single column vector – Fig. 1) - the frequency plane was divided into 5 bins and the time plane into 10) was still quite high, leading to some misclassification of cases. Therefore, a second dimensionality reduction stage relying on PCA [17] was employed before the application of the classifier.

For the classification stage a simple linear minimum distance classifier [18] was selected. The minimum Mahalanobis distance classifier assumes normal distributed values and furthermore during the estimation of the covariance matrix $\mathbf{C}$ (equation (5)) it assumes that it is constant across all the classes. Within this setting, each feature vector $\mathbf{x}$ is assigned to class i^* (normal, one broken bar, two broken bars) such that the value of the corresponding discriminant function is maximized:

$$i^* = \arg\max_i \left\{ 2\ln P(\omega_i) - (\mathbf{x}-\boldsymbol{\mu}_i)^T \mathbf{C}^{-1} (\mathbf{x}-\boldsymbol{\mu}_i) \right\}, \qquad (5)$$

where $\boldsymbol{\mu}_i$ is the mean of class i, $P(\omega_i)$ is the prior probability of class i, and $\mathbf{C}$ is the estimated covariance matrix.

The number of the retained principal components was set equal to four after inspecting the scree plot (Fig. 7) for the simulated data and for comparison reasons also three and five components were also tested. The same setting was adopted also for the experimental data.

For the case of the simulated data, a 10 fold cross validation procedure was performed making sure that recordings coming from the same start-up were always put in the same fold [19]. For the experimental data, a leave one startup recording out procedure was used, meaning that each time the three recordings of one startup experiment were left out for testing while all the rest startups were used for training.

The results are summarized in the following Tables I to VI which depict the confusion matrix for the three different configurations of the principal components. (Note: a confusion matrix is a sort of contingency table containing information about actual and predicted classifications done by a classification system. The name stems from the fact that it makes it easy to see if the classifier confuses the different classes. The columns are labeled with the predicted classes and the rows with the actual/true classes (or vice versa) and each entry (i, j) in the matrix denotes the number of cases that actually belong to class i and have been assigned to class j. For example, in Table I, the entry in row three, column two indicates that two cases that actually belonged to the two broken bar category were mistakenly classified (estimated) as belonging to the one broken bar category. The better the classifier the less non-zero off-diagonal elements exist, with the perfect classification system corresponding to a diagonal matrix).

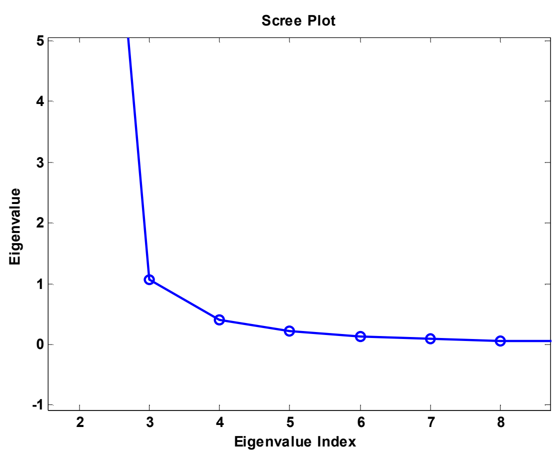

Figure 7. The scree plot (zoomed in) for the simulation data. A reasonable selection for the number of retained components is 4, where the elbow occurs.

TABLE I. CONFUSION MATRIX FOR THE SIMULATED DATA FOR THE CASE OF THREE RETAINED PRINCIPAL COMPONENTS

		Estimated class		
		Healthy	***1 BB***	***2 BB***
True class	***Healthy***	30	0	0
	1BB	0	30	0
	2BB	0	2	28

TABLE II. CONFUSION MATRIX FOR THE SIMULATED DATA FOR THE CASE OF FOUR RETAINED PRINCIPAL COMPONENTS

		Estimated class		
		Healthy	***1 BB***	***2 BB***
True class	***Healthy***	30	0	0
	1BB	0	30	0
	2BB	0	0	30

TABLE III. CONFUSION MATRIX FOR THE SIMULATED DATA FOR THE CASE OF FIVE RETAINED PRINCIPAL COMPONENTS

		Estimated class		
		Healthy	***1 BB***	***2 BB***
True class	***Healthy***	30	0	0
	1BB	0	30	0
	2BB	0	0	30

TABLE IV. CONFUSION MATRIX FOR THE EXPERIMENTAL DATA FOR THE CASE OF THREE RETAINED PRINCIPAL COMPONENTS

		Estimated class		
		Healthy	***1 BB***	***2 BB***
True class	***Healthy***	12	0	0
	1BB	0	12	0
	2BB	0	0	12

TABLE V. CONFUSION MATRIX FOR THE EXPERIMENTAL DATA FOR THE CASE OF FOUR RETAINED PRINCIPAL COMPONENTS

		Estimated class		
		Healthy	***1 BB***	***2 BB***
True class	***Healthy***	12	0	0
	1BB	0	12	0
	2BB	0	0	12

TABLE VI. CONFUSION MATRIX FOR THE EXPERIMENTAL DATA FOR THE CASE OF FIVE RETAINED PRINCIPAL COMPONENTS

		Estimated class		
		Healthy	***1 BB***	***2 BB***
True class	***Healthy***	12	0	0
	1BB	0	12	0
	2BB	0	0	12

As it can be seen from the confusion matrices, the method is very effective and only in the case of three principal components for the simulated data it erroneously diagnoses two cases with two broken bars as having only one broken bar. However even in that case it still does not mix the healthy with the faulty cases.

This can be further illustrated if we depict the projection of the PAA data onto the first three principal components (Fig. 8). As it can be seen, the healthy/normal operating data are lying far apart from the faulty cases, whereas the two faulty cases are at some areas quite close in this reduced feature space.

IV. CONCLUSIONS

In this work a computationally efficient method for the diagnosis of broken bars during the startup was presented. The proposed method employs a steady state detector for the isolation of the transient and then relies on the well-known STFT for the derivation of the time-frequency representation of the transient.

This transformation results in high dimensional representation which needs further processing in order to overcome the curse of dimensionality. For this part the 2dimensional variant of the PAA, which is a very popular method in the time series data mining field for dimensionality reduction, was employed. Aggregation is a popular method in data mining for the reduction of the input dimension and it can increase generalization even though initially it seems to lead to loss of information [20].

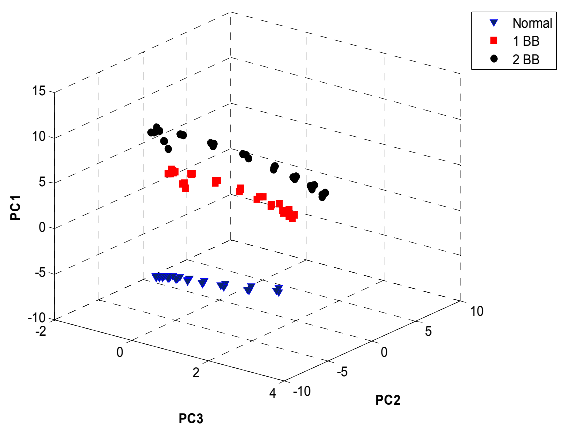

Figure 8. Projection of the simulated data onto the first three principal axes. With blue triangles are depicted the normal oprating data and with red rectangles and black sircles the one broken bar and the two broken bar cases repsectively.

The PAA representation is further reduced using PCA and then the output of the PCA stage is fed to a simple linear classifier which performs the diagnosis.

Our initial investigation indicates the good potential of the method, which is very appealing due to its very low computational overhead.

The main limitation of our method as all data driven ones is that it requires the use of training data from all the involved fault classes.

In future work we will test our method using data coming from other machines as well as for the diagnosis of other faults apart from broken bars.

REFERENCES

[1] F. Filippetti, G. Franceschini, C. Tassoni, and P. Vas, "Recent developments of induction motor drives fault diagnosis using AI techniques," *IEEE Transactions on Industrial Electronics*, vol. 47, vo. 5, pp 994-1004, October 2000.

[2] S. H. Kia, H. Henao, and G. Capolino, "Efficient digital signal processing techniques for induction machines fault diagnosis," *in proc. of the 2013 IEEE Workshop on Electrical Machines Design Control and Diagnosis (WEMDCD)*, pp. 232-246, 11-12 March 2013.

[3] J. Pons-Llinares, V. Climente-Alarcón, F. Vedreño-Santos, J. Antonino-Daviu, and M. Riera-Guasp, "Electric Machines Diagnosis Techniques via Transient Current Analysis," *in Proceedings of the 38th Annual Conference of the IEEE Industrial Electronics Society, IECON 2012*, 25-28 October, 2012, Montreal, Canada.

[4] P. Zhang, Y. Du, T.G. Habetler, and B. Lu, "A Survey of Condition Monitoring and Protection Methods for Medium-Voltage Induction Motors," *IEEE Transactions on Industry Applications,* vol.47, no.1, pp.34,46, Jan.-Feb. 2011.

[5] J. Faiz, V. Ghorbanian, and B. M. Ebrahimi, "A survey on condition monitoring and fault diagnosis in line-start and inverter-fed broken bar induction motors," *in proc. of the 2012 IEEE International Conference on Power Electronics, Drives and Energy Systems (PEDES)*, pp.1,5, 16-19 Dec. 2012.

[6] W. T. Thomson, and M. Fenger, "Current signature analysis to detect induction motor faults" *IEEE Industry Applications Magazine,* pp. 26-34, July/August 2001

[7] R. R. Schoen and T.G. Habetler. "Evaluation and Implementation of a System to Eliminate Arbitrary Load Effects in Current-Based Monitoring of Induction Machines," *IEEE Trans. Ind. Appl.,* vol.33, no. 6, pp. 1571-1577, November/December 1997.

[8] J. A. Antonino-Daviu, M. Riera-Guasp, J. R. Folch, and M. Pilar Molina Palomares, "Validation of a new method for the diagnosis of rotor bar failures via wavelet transform in industrial induction machines," *IEEE Trans. Ind. Appl.,* vol. 42, pp. 990-996, 2006.

[9] J. Park, B. Kim, J. Yang, K. Lee, S.B. Lee, E.J. Wiedenbrug, M. Teska, and S. Han, "Evaluation of the Detectability of Broken Rotor Bars for Double Squirrel Cage Rotor Induction Motors," *in proc. of the IEEE ECCE,* pp. 2493-2500, Sept. 2010.

[10] M. Riera-Guasp, J. A. Antonino-Daviu, M. Pineda-Sanchez, R. Puche-Panadero, and J. Perez-Cruz, "A General Approach for the Transient Detection of Slip-Dependent Fault Components Based on the Discrete Wavelet Transform," *IEEE Trans. Ind. Electron.*, vol. 55, pp. 4167-4180, 2008.

[11] J. Antonino-Daviu, S. Aviyente, E. Strangas, M. Riera, "A Scale Invariant Algorithm for the Automatic Diagnosis of Rotor Bar Failures in Induction Motors", *IEEE Transactions on Industrial Informatics*, vol. 9, no.1, pp. 100-108, Feb. 2013.

[12] E. Keogh, K. Chakrabarti, M. Pazzani, and S. Mehrotra, "Locally adaptive dimensionality reduction for indexing large time series databases," In *ACM SIGMOD Record,* vol. 30, no. 2, pp. 151-162, May 2001.

[13] B. K ,Yi and C. Faloutsos, "Fast time sequence indexing for arbitrary Lp norms," *in proc. of the VLDB*., 2000.

[14] G. Georgoulas, I. P Tsoumas, J. A. Antonino-Daviu, V. Climente-Alarcón, C. D. Stylios, E. D. Mitronikas, and A. N. Safacas "Automatic pattern identification based on the Complex Empirical Mode Decomposition of the startup current for the diagnosis of rotor asymmetries in asynchronous machines," *IEEE Transactions on Industrial Electronics*, vol. 61, vo. 9, pp 4937 - 4946, September 2014.

[15] P. Karvelis, I. P. Tsoumas, G. Georgoulas, C. D. Stylios, J. A. Antonino-Daviu, and V. Climente-Alarcon, (2013, November). An intelligent icons approach for rotor bar fault detection. In *Industrial Electronics Society, IECON 2013-39th Annual Conference of the IEEE,* pp. 5526-5531, 2013

[16] J. Chen, Y. S. Moon, M. F. Wong, and G. Su, "Palmprint authentication using a symbolic representation of images," *Image and Vision Computing*, vol. 28, no. 3, 343-351, 2010

[17] I. Jolliffe, *Principal component analysis*. John Wiley & Sons, Ltd., 2005

[18] R. O. Duda, P. E. Hart, and D. G. Stork, *Pattern classification*. John Wiley & Sons, 2002

[19] N. Japkowicz, and M. Shah, Evaluating learning algorithms: a classification perspective. Cambridge University Press, 2011.

[20] T. Pang-Ning, M. Steinbach, and V. Kumar, V. (2006). Introduction to data mining. In *Library of Congress*.